J|A|C|S
ARTICLES
Published on Web 08/31/2002

Solution and Solid-State Models of Peptide CH···O Hydrogen Bonds

Paul W. Baures,* Alicia M. Beatty,† Muthu Dhanasekaran,‡ Brian A. Helfrich, Waleska Pérez-Segarra, and John Desper

Contribution from the Department of Chemistry, 111 Willard Hall, Kansas State University, Manhattan, Kansas 66506

Received January 28, 2002

Abstract: Fumaramide derivatives were analyzed in solution by ^{1}H NMR spectroscopy and in the solid state by X-ray crystallography in order to characterize the formation of CH···O interactions under each condition and to thereby serve as models for these interactions in peptide and protein structure. Solutions of fumaramides at 10 mM in $CDCl_3$ were titrated with DMSO-d_6, resulting in chemical shifts that moved downfield for the CH groups thought to participate in CH···O═S$(CD_3)_2$ hydrogen bonds concurrent with NH···O═S$(CD_3)_2$ hydrogen bonding. In this model, nonparticipating CH groups under the same conditions showed no significant change in chemical shifts between 0.0 and 1.0 M DMSO-d_6 and then moved upfield at higher DMSO-d_6 concentrations. At concentrations above 1.0 M DMSO-d_6, the directed CH···O═S$(CD_3)_2$ hydrogen bonds provide protection from random DMSO-d_6 contact and prevent the chemical shifts for participating CH groups from moving upfield beyond the original value observed in $CDCl_3$. X-ray crystal structures identified CH···O═C hydrogen bonds alongside intermolecular NH···O═C hydrogen bonding, a result that supports the solution ^{1}H NMR spectroscopy results. The solution and solid-state data therefore both provide evidence for the presence of CH···O hydrogen bonds formed concurrent with NH···O hydrogen bonding in these structures. The CH···O═C hydrogen bonds in the X-ray crystal structures are similar to those described for antiparallel β-sheet structure observed in protein X-ray crystal structures.

Introduction

Hydrogen bonding in biological systems has long been associated with contributing to the structure and function of biomolecules.[1] The participation of C−H bonds in the formation of intermolecular complexes to electron donor atoms has been long established,[2−4]although disagreements regarding the nature of these interactions persist today.[5−7] In general, these interactions are described as CH···O hydrogen bonds for which Steiner[8] has recently proposed the following definition:

An X−H···A interaction is called a "hydrogen bond" if (1) it constitutes a local bond and (2) X−H acts as a proton donor to A.

Hydrogen-bond energies can vary from 0.2 to 40 kcal/mol and include contributions from electrostatic, polarization, charge transfer, dispersion, and exchange repulsion forces.[8] These individual energies can contribute different percentages toward the total energy of a hydrogen bond, especially when strong, partially covalent hydrogen bonds (15−40 kcal/mol) are considered vs those that are moderate (4−15 kcal/mol) or weak (<4 kcal/mol).[8] Generally, distance and angle criteria are used to classify heteroatom contacts as hydrogen bonds. For weak hydrogen bonds such as those described by CH···O contacts, the distance between the carbon and oxygen atoms are generally shorter than the sum of their van der Waals (vdW) radii [3.25 Å] and the angles at both the hydrogen and the oxygen are greater than 110°.[8−11] It has been pointed out, however, that these geometric criteria are far too restrictive and should no longer be applied.[8] Indeed, there are examples of CH···O contacts that either do not fit these geometric criteria[6,10,12,13] or do not show the spectroscopic changes expected for hydrogen-bonded atoms.[14]

In recent years there has been mounting evidence regarding the importance of CH···O hydrogen bonds in peptide and protein structure.[5,15−29] The presence of CH···O hydrogen bonds in antiparallel β-sheets (Figure 1) has been acknowledged on the

* Corresponding author: e-mail baures@signaturebio.com. Present address: Signature Bioscience, Inc., 1240 South 27th Street, Richmond, CA 94804.
† Present address: University of Notre Dame.
‡ Present address: University of Arizona.

(1) Jeffrey, G. A.; Saenger, W. In *Hydrogen Bonding in Biological Structures*; Springer-Verlag: New York, 1991.
(2) Sutor, D. J. *Nature* **1962**, *195*, 68−69.
(3) Allerhand, A.; Schleyer, P. v. R. *J. Am. Chem. Soc.* **1963**, *85*, 1715−1723.
(4) Green, R. D. In *Hydrogen Bonding by C−H Groups*; John Wiley & Sons: New York, 1974.
(5) Steiner, T. *J. Chem. Soc., Perkin Trans. 2* **1995**, 1315−1319.
(6) Steiner, T.; Desiraju, G. R. *J. Chem. Soc., Chem. Commun.* **1998**, 891−892.
(7) Dunitz, J. D.; Gavezzotti, A. *Acc. Chem. Res.* **1999**, *32*, 677−684.
(8) Steiner, T. *Angew. Chem., Int. Ed.* **2002**, *41*, 48−76.
(9) Desiraju, G. R.; Steiner, T. In *The Weak Hydrogen Bond in Structural Chemistry and Biology*; Desiraju, G. R., Steiner, T., Eds.; Oxford University Press: New York, 1999.
(10) Taylor, R.; Kennard, O. *Acc. Chem. Res.* **1984**, *17*, 320−326.
(11) Taylor, R.; Kennard, O. *J. Am. Chem. Soc.* **1982**, *104*, 5063−5070.
(12) Gavezzotti, A. *Crystallogr. Rev.* **1998**, *7*, 5−121.
(13) Steiner, T.; Saenger, W. *J. Chem. Soc., Perkin Trans. 2* **1998**, 371−377.
(14) Chaney, J. D.; Goss, C. R.; Folting, K.; Santarsiero, B. D.; Hollingsworth, M. D. *J. Am. Chem. Soc.* **1996**, *118*, 9432−9433.

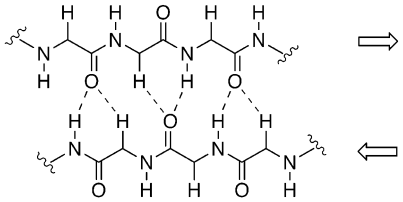

Figure 1. Antiparallel β-sheet structure illustrating concurrent NH···O and CH···O hydrogen bonds.

basis of X-ray crystal structures where the distances between heteroatoms were used in their identification.[21,23] In this manner, the CH···O hydrogen bond has also been shown to be involved in the capping of α-helices in several peptide sequences that terminate in the Schellman motif[28] and in a peptide containing a γ-amino acid that forms an intramolecular CH···O hydrogen bond reminiscent of a hydrogen-bonded β-turn conformation.[29] It is reasonable to expect that foldamers containing unnatural amino acids will also utilize CH···O hydrogen bonds as stabilizing elements of their secondary structure.[30−37] Ab initio studies of formamide dimers have been used to estimate a possible energetic contribution of CH···O hydrogen bonds in protein structure.[19] These calculations suggest that CH···O hydrogen bonds could be significant contributors to protein folding and structure due to their individual contribution to stability as well as the large number of contacts common in a typical protein. To date, there have been no experimental quantifications of CH···O hydrogen-bond energies.

Early solution studies of C−H group interactions often employed freezing-point depression, enthalpies of mixing, vibrational spectroscopy, and NMR spectroscopy in order to verify and characterize the formation of complexes.[4] For example, the chloroform ^{1}H NMR signal in acetone, ethyl ether, or triethylamine is found downfield in comparison to a nonpolar medium such as cyclohexane, a result consistent with the formation of CH···O hydrogen bonds to the polar solvents.

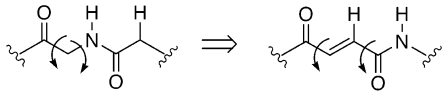

Figure 2. Similarities of an *N*-acylpeptide with a fumaramide derivative in the s-cis, s-cis conformation, including two rotatable bonds and both NH and CH groups adjacent to a carbonyl group.

The CH···O hydrogen bond has been used in crystal engineering[38−41] and has also been described in the context of drug design and molecular recognition.[1,9,42−45] Yet it has rarely been used in the deliberate design of biologically active compounds.[46,47] We are unaware of any reports to date suggesting the presence of CH···O hydrogen bonds in the peptoids [*N*-alkylglycine oligomers], though the similar bioactivity[48−51] and secondary structures observed for some peptoids as compared to the corresponding peptide sequences is noteworthy.[52−55] In designing these oligomers, a peptide is aligned with the retropeptoid backbone in a manner that superimposes the carbonyl groups and the side chains of each structure. This alignment effectively replaces the NH groups in the peptide backbone for backbone CH_2 groups in the peptoid.

This paper describes the use of fumaramides as models of the peptide bond (Figure 2) that are useful for studying CH···O hydrogen bonds in both solution and the solid state. The fumaramide reverses the position of the strong hydrogen-bond donor (NH) and the associating CH group as compared with an *N*-acylpeptide bond. Though the fumaramide retains two rotatable bonds, the s-cis and s-trans orientations are recognized as nearly equivalent in energy and of lower energy than other noncoplanar bond orientations.[56] Thus, it was expected that the

(15) Senes, A.; Ubarretxena-Belandia, I.; Engelman, D. M. *Proc. Natl. Acad. Sci. U.S.A.* **2001**, *98*, 9056−9061.
(16) Felcy Fabiola, G.; Bobde, V.; Damodharan, L.; Pattabhi, V.; Durani, S. *J. Biomol. Struct. Dyn.* **2001**, *18*, 579−594.
(17) Olson, C. A.; Shi, Z.; Kallenbach, N. R. *J. Am. Chem. Soc.* **2001**, *123*, 6451−6452.
(18) Thakur, A. K.; Kishore, R. *Biopolymers* **2000**, *53*, 447−454.
(19) Vargas, R.; Garza, J.; Dixon, D. A.; Hay, B. P. *J. Am. Chem. Soc.* **2000**, *122*, 4750−4755.
(20) Nagarajan, V.; Pattabhi, V.; Johnson, A.; Bobde, V.; Durani, S. *Int. J. Pept. Protein Res.* **1997**, *49*, 74−79.
(21) Fabiola, G. F.; Krishnaswamy, S.; Nagarajan, V.; Pattabhi, V. *Acta Crystallogr. D* **1997**, *53*, 316−320.
(22) Bella, J.; Berman, H. M. *J. Mol. Biol.* **1996**, *264*, 734−742.
(23) Derewenda, Z. S.; Lee, L.; Derewenda, U. *J. Mol. Biol.* **1995**, *252*, 248−262.
(24) Panneerselvam, K.; Chacko, K. K. *Int. J. Pept. Protein Res.* **1990**, *35*, 460−464.
(25) Panneerselvam, K.; Chacko, K. K.; Veena, R. *Int. J. Pept. Protein Res.* **1989**, *33*, 191−194.
(26) Parthasarathy, R.; Fridey, S. M.; Srikrishnan, T. *Int. J. Pept. Protein Res.* **1989**, *33*, 308−312.
(27) Ramachandran, G. N.; Chanrasekharan, R. *Biopolymers* **1968**, *6*, 1649−1658.
(28) Aravinda, S.; Shamala, N.; Pramanik, A.; Das, C.; Balaram, P. *Biochem. Biophys. Res. Commun.* **2000**, *273*, 933−936.
(29) Cheung, E. Y.; McCabe, E. E.; Harris, K. D. M.; Johnston, R. L.; Tedesco, E.; Raja, K. M. P.; Balaram, P. *Angew. Chem., Int. Ed.* **2002**, *41*, 494−496.
(30) Seebach, D.; Brenner, M.; Rueping, M.; Bernhard, J. *Chemistry* **2002**, *8*, 573−584.
(31) Etezady-Esfarjani, T.; Hilty, C.; Wuethrich, K.; Rueping, M.; Schrieber, J. Seebach, D. *Helv. Chim. Acta* **2002**, *85*, 1197−1209.
(32) Hill, D. J.; Mio, M. J.; Prince, R. B.; Hughes, T. S.; Moore, J. S. *Chem. Rev.* **2001**, *101*, 3893−4011.
(33) Woll, M. G.; Lai, J. R.; Guzei, I. A., Taylor, S. J. C.; Smith, M. E. B.; Gellman, S. H. *J. Am. Chem. Soc.* **2001**, *123*, 11077−11078.
(34) Cheng, R. P.; Gellman, S. H.; DeGrado, W. F. *Chem. Rev.* **2001**, *101*, 3219−3232.
(35) Abele, S.; Vogtli, K.; Seebach, D. *Helv. Chim. Acta* **1999**, *82*, 1539−1558.
(36) Gellman, S. H. *Acc. Chem. Res.* **1998**, *31*, 173−180.
(37) Seebach, D.; Matthews, J. L. *Chem. Commun.* **1997**, 2015−2022.
(38) Anthony, A.; Desiraju, G. R.; Jetti, R. K. R.; Kuduva, S. S.; Madhavi, N. N. L.; Nangia, A.; Thaimattam, R.; Thalladi, V. R. *Cryst. Eng.* **1998**, *1*, 1−18.
(39) Desiraju, G. R. *Acc. Chem. Res.* **1996**, *29*, 441−449.
(40) Desiraju, G. R. *Angew. Chem., Int. Ed. Engl.* **1995**, *34*, 2311−2327.
(41) Aakeröy, C. B. *Acta Crystallogr.* **1997**, *B53*, 569−586.
(42) Burley, S. K.; Petsko, G. A. *Adv. Protein Chem.* **1988**, *39*, 125−189.
(43) Wahl, M. C.; Sundaralingam, M. *Trends Biochem. Sci.* **1997**, *22*, 97−102.
(44) Pascard, C. *Acta Crystallogr.* **1995**, *D51*, 407−417.
(45) Glusker, J. P. *Acta Crystallogr.* **1995**, *D51*, 418−427.
(46) Baures, P. W.; Wiznycia, A. V.; Beatty, A. M. *Bioorg. Med. Chem.* **2000**, *8*, 1599−1605.
(47) Baures, P. W. *Org. Lett.* **1999**, *1*, 249−252.
(48) Low, C. M. R.; Black, J. W.; Broughton, H. B.; Buck, I. M.; Davies, J. M. R.; Dunstone, D. J.; Hull, R. A. D.; Kalindjian, S. B.; McDonald, I. M.; Pether, M. J.; Shankley, N. P.; Steel, K. I. M. *J. Med. Chem.* **2000**, *43*, 3505−3517.
(49) Heizmann, G.; Hildebrand, P.; Tanner, H.; Ketterer, S.; Pansky, A.; Froidevaux, S.; Beglinger, C.; Eberle, A. N. *J. Recept. Signal Transduct. Res.* **1999**, *19*, 449−466.
(50) Tran, T.-A.; Mattern, R.-H.; Afargan, M.; Amitay, O.; Ziv, O.; Morgan, B. A.; Taylor, J. E.; Hoyer, D.; Goodman, M. *J. Med. Chem.* **1998**, *41*, 2679−2685.
(51) Figliozzi, G. M.; Goldsmith, R.; Ng, S. C.; Banville, S. C.; Zuckermann, R. N. *Methods Enzymol.* **1996**, *267*, 437−447.
(52) Armand, P.; Kirshenbaum, K.; Goldsmith, R. A.; Farr-Jones, S.; Barron, A. E.; Truong, K. T. V.; Dill, K. A.; Mierke, D. F.; Cohen, F. E.; Zuckermann, R. N.; Bradley, E. K. *Proc. Natl. Acad. Sci., U.S.A.* **1998**, *95*, 4309−4314.
(53) Kirshenbaum, K.; Barron, A. E.; Goldsmith, R. A.; Armand, P.; Bradley, E. K.; Truong, K. T. V.; Dill, K. A.; Cohen, F. E.; Zuckermann, R. N. *Proc. Natl. Acad. Sci., U.S.A.* **1998**, *95*, 4303−4308.
(54) Armand, P.; Kirshenbaum, K.; Falicov, A.; Dunbrack, R. I., Jr.; Dill, K. A.; Zuckermann, R. N.; Cohen, F. E. *Folding Des.* **1997**, *2*, 369−375.
(55) Sanborn, T. J.; Wu, C. W.; Zuckerman, R. N.; Barron, A. E. *Biopolymers* **2002**, *63*, 12−20.
(56) Eliel, E. L.; Wilen, S. H.; Doyle, M. P. In *Basic Organic Stereochemistry*; Eliel, E. L., Wilen, S. H., Doyle, M. P., Eds.; John Wiley & Sons: New York, 2001; p 394.

Scheme 1

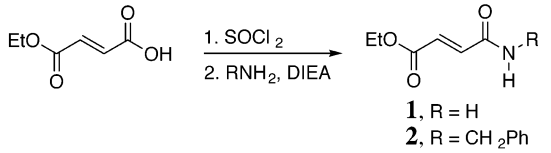

Scheme 2

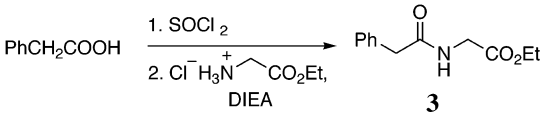

Chart 1. Starting Materials Used for Library Synthesis

carboxylic acids

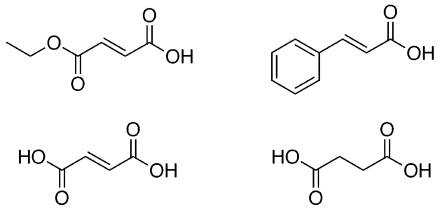

α-amino acids

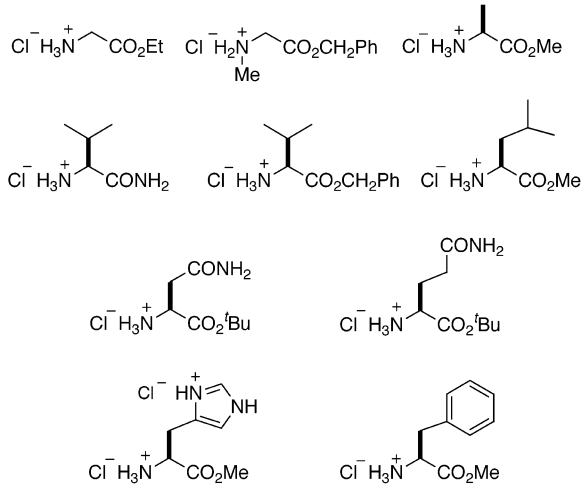

fumaramides could form concurrent NH···O and CH···O hydrogen bonds in solutions containing strong hydrogen-bond acceptors such as DMSO-d_6. The solid-state packing of fumaramides was expected to result from concurrent NH···O and CH···O hydrogen bonds and we report herein the solid-state structures of a peptide, two comparative fumaramides, and two additional model compounds.

Results and Discussion

Synthesis. The synthesis of **1** and **2** were accomplished from monoethyl fumarate via the acid chloride (Scheme 1). Similarly, the peptide analogue **3** was synthesized by first forming the acid chloride of phenylacetic acid and then reacting this intermediate with glycine ethyl ester hydrochloride and diisopropylethylamine (Scheme 2). As a means to identify crystalline derivatives that could be added to this study, a library of 40 compounds was synthesized in parallel fashion by using two monocarboxylic acids and two dicarboxylic acids and combining these with 10 different amino acid derivatives (Chart 1). Solutions of the starting materials in ethanol were mixed with *N*-methylmorpholine and an aqueous solution of a water-soluble carbodiimide. Solids formed in some of the reaction vials as the solutions were allowed to concentrate to approximately half of the initial volume. Crystallization of products **4**−**7** was observed and these compounds were then synthesized on a larger scale for detailed analysis (Chart 2).

Chart 2

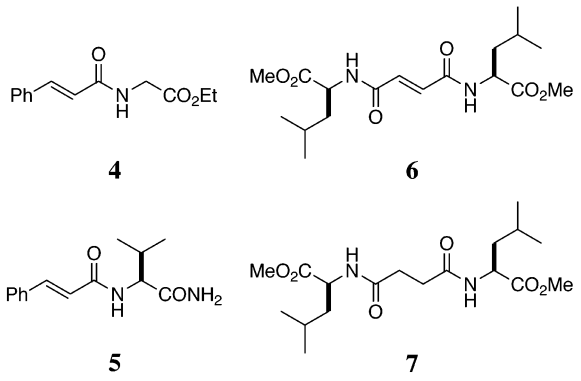

Chart 3

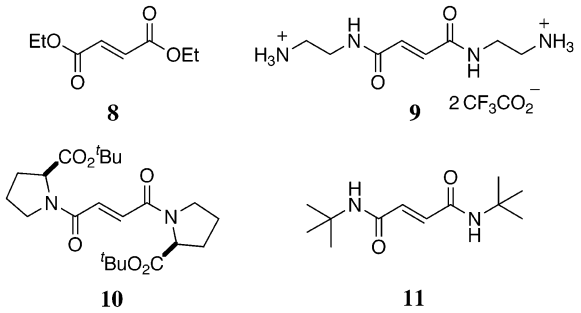

Table 1. Alkene CH Chemical Shift Comparisons[a]

compound	observed[b]	calculated[c]
1	6.96, 6.83	7.63, 7.01
	6.96, 6.56	
2	6.90, 6.85	7.63, 7.01
	7.06, 6.62	
4	7.66, 6.47	7.61, 6.98
	7.46, 6.72	
6	6.90	7.60
	6.90	
8	6.85	7.04
	6.71	
9	6.90[d]	7.60
10	7.29, 7.08[e]	7.60
11	7.97[f]	7.60

[a] Chemical shifts are in parts per million (ppm). [b] Values were determined at a concentration of 10 mM (**1**−**8**) in $CDCl_3$ or DMSO-d_6 (values shown in italic type). [c] Reference 58. [d] D_2O, ref 59. [e] $CDCl_3$, ref 60. [f] DMSO-d_6, ref 61.

Solution ^{1}H NMR Studies. We attempted to make initial alkene CH chemical shift assignments for **1**, **2**, and **4** on the basis of standard chemical shift models for substituted ethylenes,[57,58] along with the addition of **8**−**11** (Chart 3) as examples for comparison. However, the observed chemical shifts are significantly different than the calculated chemical shifts based on these models (Table 1). There are also differences in the alkene chemical shift depending upon the solvent, although only one of the two alkene CHs in each of the compounds **1**, **2**, and **4** shifts dramatically upfield in DMSO-d_6 as compared to $CDCl_3$.

(57) Pascual, C., Meier, J.; Simon, W. *Helv. Chim. Acta* **1966**, *49*, 164−168.
(58) Matter, U. E.; Pascual, C.; Pretsch, E.; Pross, A.; Simon, W.; Sternhell, S. *Tetrahedron* **1969**, *25*, 691−697.

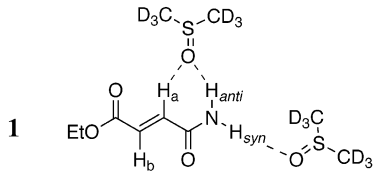

Figure 3. Hydrogen bonding (NH···O) of **1** to DMSO-d_6 with a concurrent CH···O hydrogen bond to H_a.

By comparison, the alkene CH in **6** is found at 6.90 ppm in both $CDCl_3$ and DMSO-d_6, a value consistent with the CH observed furthest downfield in **1** and **2**. Diethyl fumarate, **8**, was also used for comparison with the alkene CH in this diester observed at 6.85 ppm in $CDCl_3$ (as well as in solution containing up to 10.0 M DMSO-d_6) and then found at 6.71 ppm in DMSO-d_6. These values are consistent with the upfield shift for one of the two alkene CHs in both **1** and **2**. Compound **9** in D_2O has an alkene chemical shift at 6.90 ppm,[59] while **10** in $CDCl_3$ has two alkene CH chemical shifts observed at 7.29 and 7.08 ppm.[60] It is likely that the two shifts are due to conformational s-cis and s-trans isomers, as two sets of ^{13}C NMR signals were also observed for **10**. The alkene chemical shift values for **1** and **2** places these compounds in a very select category since the deviations between observed and predicted values are greater than 0.50 ppm—a category into which only 0.3% of 4298 alkenes fell in an early compilation.[58] Compound **11**, though very similar to **6** and **9** in structure, has an alkene chemical shift significantly higher and closer to its predicted value.[61] We do not have a satisfactory explanation for the chemical shift behavior of these alkenes at this time, although similar α,β-unsaturated systems also have alkene chemical shift values disparate from those calculated on the basis of the earlier models.[62−65]

Confirmation of the alkene chemical shift assignments was attempted by using NOESY NMR spectroscopy on solutions of **1** and **2** in $CDCl_3$ containing 100 mM and 1.0 M DMSO-d_6, respectively, and looking for the $NH_{anti}-H_a$ (or comparable) nuclear Overhauser effect (NOE) cross-peak. Fumaramides **1** and **2** were expected to associate with a strong hydrogen-bond acceptor and thereby result in an observable effect on the NH and CH chemical shift values (Figure 3). Unfortunately, we were unable to observe any cross-peaks from an NH to either alkene CH, presumably due to rapid bond rotation on the NMR time scale that occurs even in the presence of the 1.0 M DMSO-d_6. The solution NMR data are therefore only supportive of the interactions shown in Figure 3, and evidence of the concurrent CH···O hydrogen bond in solution is not definitive at this time. The extent to which these data do support the presence of this CH···O hydrogen bond over other possibilities, such as solvent polarity and conformation as previously described for α,β-unsaturated carbonyl compounds,[66] is included in the following descriptions of chemical shift behavior for each compound measured as a function of increasing DMSO-d_6 concentration.

Table 2. Chemical Shift Values of **1**[a] Observed in Varying Proportions of $CDCl_3$ and DMSO-d_6

[DMSO-d_6]	NH_{anti}	NH_{syn}	H_a[b]	H_b[b]
0.00 mM	5.66	5.66	6.96	6.83
5.00 mM	5.69	5.69	6.94	6.83
10.0 mM	5.69	5.69	6.94	6.83
20.0 mM	5.75	5.75	6.94	6.84
50.0 mM	5.81	5.81	6.95	6.84
100 mM	6.40	6.02	6.98	6.84
200 mM	6.64	6.06	7.00	6.83
500 mM	7.00	6.12	7.03	6.82
1.00 M	7.16	6.16	7.04	6.80
10.0 M	7.86	7.42	6.98	6.58
14.1 M	7.90	7.51	6.96	6.56

[a] Compound **1** (10 mM): $Et_2OC-CH_b=CH_a-CONH_2$. Chemical shifts are in parts per million. [b] Alkene chemical shift assignments are tentative as discussed in the text.

The $CDCl_3$ solutions containing DMSO-d_6 were referenced to tetramethylsilane (TMS) since the observed $CHCl_3$ and DMSO chemical shift values are dependent upon the concentration of one another. The chemical shift of $CHCl_3$ was observed at 7.26(2) ppm in the solutions containing 0.0−1.0 M DMSO-d_6, 8.19(3) ppm at 10.0 M DMSO-d_6, and 8.31(2) ppm in the 14.1 M DMSO-d_6 solutions. Trace $CHCl_3$ in DMSO-d_6 is observed at 8.32 ppm.[67]

When a 10 mM solution of **1** in $CDCl_3$ is titrated with DMSO-d_6, a downfield shift for the amide NH resonance is observed due to hydrogen bonding with the DMSO-d_6 (Table 2). Two amide NH resonances are observed at and above 100 mM DMSO-d_6, while at low concentrations of DMSO-d_6 (<100 mM) the NH chemical shift values are identical to one another due to either the fast dynamics of bond rotation at room temperature or coincidence. Increasing the concentration of a strong hydrogen-bond acceptor such as DMSO-d_6 could be expected to slow bond rotation due to the additional energetic penalty of breaking this hydrogen bond, though the on and off rate of DMSO-d_6 hydrogen-bond formation could still be fast on the NMR time scale. The higher DMSO-d_6 concentrations may have an additional influence on the kinetics of bond rotation due to the significant change in solvent polarity over the $CDCl_3$ solutions. If the chemical shift of the carboxamide NHs are identical due to coincidence, then increasing the concentration of DMSO-d_6 could still differentiate the NHs due to the alternate environments formed in the hydrogen-bonded complex. The alkene and amide hydrogen chemical shift data for **1** from the 0.0−1.0 M DMSO-d_6 solutions is graphed in Figure 4. The amide NH chemical shifts have the greatest frequency separation (1.00 ppm) at 1.0 M DMSO-d_6 in the solutions tested, but the separations in 10.0 M DMSO-d_6 (0.44 ppm) and in neat DMSO-d_6 (0.39 ppm) are significantly less.

Though the NH chemical shift value for **1** changes at DMSO-d_6 concentrations below 100 mM, there are no significant changes in either alkene CH chemical shifts in these solutions. Concurrent formation of a CH···O hydrogen bond along with the NH_{anti}···O hydrogen bond is suggested at concentrations between 100 mM and 1.0 M DMSO-d_6 as evidenced by the downfield chemical shift of H_a at the same time that H_b is not

(59) Arora, P. S.; Van, Q. N.; Famulok, M.; Shaka, A. J.; Nowick, J. S. *Bioorg. Med. Chem.* **1998**, *6*, 1421−1428.
(60) Bläser, E.; Kolar, P.; Fenske, D.; Goesmann, H.; Waldmann, H. *Eur. J. Org. Chem.* **1999**, 329−333.
(61) König, S.; Lohberger, S.; Ugi, I. *Synthesis* **1993**, 1233−1234.
(62) Suhara, Y.; Maruyama, H. B.; Kotoh, Y.; Miyasaka, Y.; Yokose, K.; Shirai, H.; Takano, K.; Quitt, P.; Lanz, P. *J. Antibiot.* **1975**, *28*, 648−655.
(63) de Pooter, H.; van Rompaey, L.; van Sumere, C. F. *Bull. Soc. Chim. Belg.* **1976**, *85*, 647−656.
(64) Canoira, L.; Rodriguez, J. G. *J. Heterocycl. Chem.* **1985**, *22*, 1511−1518.
(65) Horne, S.; Taylor, N.; Collins, S.; Rodrigo, R. *J. Chem. Soc., Perkin Trans. 1* **1991**, 3047−3051.
(66) Savin, V. I.; Temyachev, I. D.; Kitaev, Y. P. *Zh. Org. Khim.* **1974**, *10*, 1590−1593.
(67) Gottlieb, H. E.; Kotlyar, V.; Nudelman, A. *J. Org. Chem.* **1997**, *62*, 7512−7515.

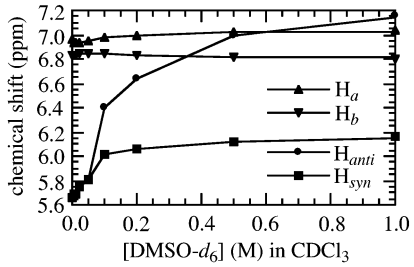

Figure 4. ^{1}H NMR chemical shift data for alkene (tentative assignments) and amide hydrogens in **1** [$Et_2OC-CH_b=CH_a-CONH_2$] as $CDCl_3$ solution containing varying concentrations of DMSO-d_6.

Table 3. Chemical Shift Values of **2**[a] Observed in Varying Proportions of $CDCl_3$ and DMSO-d_6

[DMSO-d_6]	CH_2	NH	H_a[b]	H_b[b]
0.00 mM	4.55	6.02	6.90	6.85
5.00 mM	4.55	6.17	6.92	6.85
10.0 mM	4.55	6.19	6.92	6.85
20.0 mM	4.55	6.23	6.92	6.85
50.0 mM	4.55	6.34	6.93	6.85
100 mM	4.54	6.60	6.95	6.85
200 mM	4.53	6.85	6.98	6.85
500 mM	4.52	7.61	7.04	6.84
1.00 M	4.50	7.98	7.07	6.83
10.0 M	4.41	8.95	7.07	6.64
14.1 M	4.39	9.02	7.06	6.62

[a] Compound **2** (10 mM): $Et_2OC-CH_b=CH_a-CONHCH_2Ph$. Chemical shifts are in parts per million. [b] Alkene chemical shift assignments are tentative as discussed in the text.

significantly affected. Higher concentrations of DMSO-d_6 (>1.0 M) result in H_b moving significantly upfield, a result that we attribute to increased frequency of largely random interactions of the H_b with the DMSO-d_6. In contrast, H_a is by and large protected from random DMSO-d_6 interactions at these high concentrations due to the specific and directional NH_{anti}···O hydrogen bond and concurrent CH···O hydrogen bond. This orientation of the DMSO-d_6 keeps the shielding cone of the carbonyl group directed at H_a. The observed chemical shift in pure DMSO-d_6 returns to the value observed in $CDCl_3$, likely due to the slight increase in random orientation of the DMSO-d_6 around H_a resulting from increased frequency of DMSO-d_6 exchange at higher concentrations. The magnitude of the difference in the alkene chemical shift values for the DMSO-d_6 versus $CDCl_3$ solutions cannot be interpreted in terms of the strength of the CH···O hydrogen bond[67] and is simply taken as a qualitative observation consistent with complex formation.

The chemical shift changes observed for **2** are similar to those observed for **1** with the NH chemical shift value moving downfield upon addition of DMSO-d_6 (Table 3). The H_a chemical shift value in **2** also moves downfield with increasing concentrations of DMSO-d_6, whereas H_b remains unchanged at DMSO-d_6 concentrations below 1.0 M and then moves upfield at higher concentrations. The maximum observed $\Delta\delta$ for H_a is 0.17 ppm in **2** as compared to a $\Delta\delta$ for H_a of 0.08 ppm in **1**. The ester CH_2 behaves similarly to H_b, with its observed chemical shift moving upfield at DMSO-d_6 equal to and above 1.0 M.

Peptide **3** was synthesized in order to determine whether chemical shift changes similar to those observed for **1** and **2** would occur with the addition of DMSO-d_6. The NH chemical shift for **3** moves downfield with DMSO-d_6 addition, in likewise fashion to the observed shift for **1** and **2** (Table 4). All three of

Table 4. Chemical Shift Values of **3**[a] Observed in Varying Proportions of $CDCl_3$ and DMSO-d_6

[DMSO-d_6]	H_2C	CH_2	NH	CH_2
0.00 mM	4.18	4.00	5.89	3.63
5.00 mM	4.18	3.99	5.92	3.64
10.0 mM	4.18	4.00	5.92	3.64
20.0 mM	4.18	3.99	5.93	3.64
50.0 mM	4.18	3.99	5.97	3.63
100 mM	4.18	3.99	5.97	3.63
200 mM	4.18	3.99	6.04	3.63
500 mM	4.18	3.98	6.32	3.63
1.00 M	4.17	3.98	6.69	3.62
10.0 M	4.10	3.84	8.38	3.50
14.1 M	4.07	3.82	8.46	3.48

[a] Compound **3** (10 mM): $H_3C\mathbf{H}_2CO_2CC\mathit{H}_2NHCOCH_2Ph$. Chemical shifts are in parts per million.

Table 5. Chemical Shift Values of **4**[a] Observed in Varying Proportions of $CDCl_3$ and DMSO-d_6

[DMSO-d_6]	CH_2	NH	CH_a[b]	CH_b[b]
0.00 mM	4.18	6.14	6.47	7.66
5.00 mM	4.18	6.16	6.47	7.66
10.0 mM	4.18	6.17	6.47	7.66
20.0 mM	4.18	6.19	6.47	7.66
50.0 mM	4.18	6.25	6.48	7.66
100 mM	4.17	6.40	6.50	7.65
200 mM	4.17	6.53	6.58	7.65
500 mM	4.15	6.94	6.57	7.64
1.00 M	4.12	7.40	6.62	7.62
10.0 M	3.97	8.49	6.71	7.46
14.1 M	3.96	8.53	6.72	7.46

[a] Compound **4** (10 mM): $EtO_2CC\mathit{H}_2NHCO-CH_a=CH_b-Ph$. Chemical shifts are in parts per million. [b] Alkene chemical shift assignments from ref 63.

the CH_2s in **3** behaved similarly to one another, with no significant chemical shift changes observed below 1.0 M DMSO-d_6 and upfield shifts observed at higher concentrations of DMSO-d_6. The lack of a similar upfield chemical shift for the benzyl CHs of **3** could result from several differences between **3** and **1** or **2**. There are two benzyl CHs in **3** and each could interact weakly with a DMSO-d_6 that hydrogen bonds to the NH group, or alternatively, the two CHs could be dynamically interchanging in such an interaction. There is also a difference in hybridization of the carbon atom adjacent to the amide carbonyl bond in **3** (sp^3) as compared with the carbon atom in **1** or **2** (sp^2), plus there is an altered conformational flexibility in **3**. The magnetic anisotropy of the nearby aromatic ring may also influence the chemical shift values in these solvent mixtures.[68,69] It is not possible at this time to identify which change is the most important or even whether all of the changes make contributions to the observed differences in solution.

The parallel syntheses were designed to identify additional model compounds for combined solution and solid-state analysis. *trans*-Cinnamic acid, monoethylfumarate, and fumaric acid were chosen as model carboxylic acids that retain an alkene CH adjacent to the amide carbonyl, whereas succinic acid was included as a model for peptides containing sp^3-hybridized carbon atoms adjacent to the amide carbonyl bond.

Independent titrations of **4** (Table 5) and **6** (Table 6) with DMSO-d_6 resulted in chemical shift changes that parallel those observed for **1** and **2**. The NH chemical shift values for each

(68) Wiley, G. R.; Miller, S. I. *J. Am. Chem. Soc.* **1972**, *94*, 3287−9293.
(69) Johnston, M. D., Jr.; Gasparro, F. P.; Kuntz, I. D., Jr. *J. Am. Chem. Soc.* **1969**, *91*, 5715−5724.

Table 6. Chemical Shift Values of **6**[a] Observed in Varying Proportions of $CDCl_3$ and DMSO-d_6

[DMSO-d_6]	α-CH	NH	H_a	E–H
0.00 mM	4.73	6.67	6.90	3.76
5.00 mM	4.73	6.69	6.90	3.76
10.0 mM	4.73	6.69	6.90	3.75
20.0 mM	4.73	6.71	6.91	3.76
50.0 mM	4.73	6.76	6.92	3.75
100 mM	4.72	6.83	6.94	3.75
200 mM	4.70	7.02	6.96	3.74
500 mM	4.67	7.45	7.00	3.73
1.00 M	4.64	7.83	7.03	3.72
10.0 M	4.40	8.75	6.92	3.65
14.1 M	4.37	8.81	6.90	3.64

[a] Compound **6** (10 mM): E-Leu-NHCOCH$_a$=CH$_{a'}$−CONH-Leu-E. Chemical shifts are in parts per million.

Table 7. Chemical Shift Values of **7**[a] Observed in Varying Proportions of $CDCl_3$ and DMSO-d_6

[DMSO-d_6]	α-CH	NH	CH_2	EH
0.00 mM	4.58	6.53	2.55	3.73
100 mM	4.57	6.67	2.56	3.73
500 mM	4.55	6.95	2.56	3.72
1.00 M	4.54	7.21	2.56	3.71
14.1 M	4.54	7.21	2.56	3.71

[a] Compound **7** (10 mM): E-Leu-NHCO−CH_2−CH_2−CONH-Leu-E. Chemical shifts are in parts per million.

compound moved downfield with increasing DMSO-d_6 concentration. From 100 mM to 1.0 M DMSO-d_6, the chemical shift for alkene H_a in **4** moves downfield. The downfield chemical shift changes continued for **4** at higher DMSO-d_6 concentrations, while in **6** the chemical shift values return to that observed in $CDCl_3$. This may be due to the need to only interact with one DMSO-d_6 molecule to create the complex and full change in **4**, while two DMSO-d_6 molecules must bind to **6** (a less favorable ternary complex) for the full effect to be observed. Other CHs in **4** and **6** did not have their chemical shift values change significantly below 1.0 M and then shifted upfield at increasing DMSO-d_6 concentrations.

Compound **5** was not studied in solution due to the low solubility of this compound in $CDCl_3$. Only a few solutions containing DMSO-d_6 were prepared and analyzed for **7** as no chemical shift differences were observed for any CHs at either 1.0 M or neat DMSO-d_6 as compared to the values in neat $CDCl_3$ (Table 7). The difference between **6** and **7** could again be due to dynamic exchange between possible CH···O hydrogen bonds, changes in hybridization, or altered conformational flexibility between the compounds.

X-ray Crystallography. The single-crystal X-ray structures of the model compounds were sought in order to determine whether CH···O hydrogen bonds formed concurrently with NH···O hydrogen bonds in the solid state. The presence of CH···O hydrogen bonds would support the solution NMR results since crystallization occurs by molecular recognition forces analogous to those governing solution interactions. The hydrogen-bond acceptor during crystallization is an amide carbonyl rather than a sulfoxide, but both have similar hydrogen-bond-accepting abilities.[70] Crystals suitable for single-crystal X-ray diffraction were obtained for **1**−**3**, **5**, and **6** and the crystal data for each structure are given in Table 8. Each compound forms concurrent intermolecular NH···O and CH···O hydrogen bonds. These intermolecular interactions are consistent with the solution NMR results and are illustrated in Figure 5. The corresponding distances and angles for these interactions are given in Table 9. Though crystalline solids formed for both **4** and **7**, the crystals were not suitable for the determination of their crystal structures.

There are two strong intermolecular interactions in **1**: the NH_{anti}···O_{amide} hydrogen bond, listed in Table 9 and illustrated in Figure 5a, as well as a second hydrogen bond between the carboxamide NH and ester carbonyl oxygen that is not shown in this illustration [NH_{syn}···O_{ester}, N···O separation = 3.00(1) Å, ∠NH···O = 168(1)°]. Formation of these two NH···O hydrogen bonds results in different planes being occupied by nearby molecules in the crystal lattice. A CH···O hydrogen bond is formed concurrent with the NH_{anti}···O_{amide} hydrogen bond. The distances between heteroatoms [C···O, 3.34(1) Å] and for the hydrogen to acceptor oxygen [H···O, 2.57(1) Å] are less than the vdW distances often used to distinguish these interactions.[8−11]

In contrast, the concurrent intermolecular NH···O and CH···O hydrogen bonds found in the crystal structure of **2** occur between molecules translated within the same plane. The NH···O hydrogen bond is longer in **2** [3.07(1) Å] as compared to **1** [2.90-(1) Å], but the CH···O hydrogen bond is shorter in **2** [3.25(1) Å] as compared to **1** [3.34(1) Å]. We attribute these differences to a compromise between the strength of the two interactions in the context of one another and the remaining crystal packing effects. Importantly, the presence of CH···O hydrogen bonds in the solid states of both **1** and **2**, despite differences in the crystal packing of each, supports the hypothesis of their

Table 8. Selected Crystal Data Collection and Refinement Data for **1**, **2**, **3**, **5**, and **6**

crystal data	**1**	**2**	**3**	**5**	**6**
formula	$C_6H_9NO_3$	$C_{13}H_{15}NO_3$	$C_{12}H_{15}NO_3$	$C_{14}H_{18}N_2O_2$	$C_{18}H_{30}N_2O_6$
weight (g mol^{-1})	143.14	233.26	221.25	246.30	370.44
crystal size (mm)	0.50 × 0.40 × 0.20	0.30 × 0.20 × 0.10	0.50 × 0.20 × 0.10	0.30 × 0.15 × 0.10	0.30 × 0.20 × 0.15
crystal system	orthorhombic	orthorhombic	orthorhombic	monoclinic	orthorhombic
space group	*Pna*2$_1$	*Pna*2$_1$	*Pna*2$_1$	*C*2	$P2_12_12_1$
a (Å)	20.880(5)	17.632(1)	9.975(2)	13.514(6)	14.440(5)
b (Å)	3.928(1)	14.097(1)	12.130(2)	4.797(2)	4.852(2)
c (Å)	8.610(2)	4.920(1)	9.553(2)	21.238(10)	27.377(11)
α (deg)	90.0	90.0	90.0	90.0	90.0
β (deg)	90.0	90.0	90.0	97.14(1)	90.0
γ (deg)	90.0	90.0	90.0	90.0	90.0
Z	4	4	4	4	4
temp (K)	203(2)	293(2)	203(2)	293(2)	293(2)
R/R_w^2 (obs data)	0.0257/0.0625	0.0436/0.0729	0.0333/0.0688	0.0400/0.0805	0.0687/0.1676
S	1.104	1.105	1.079	1.128	0.977

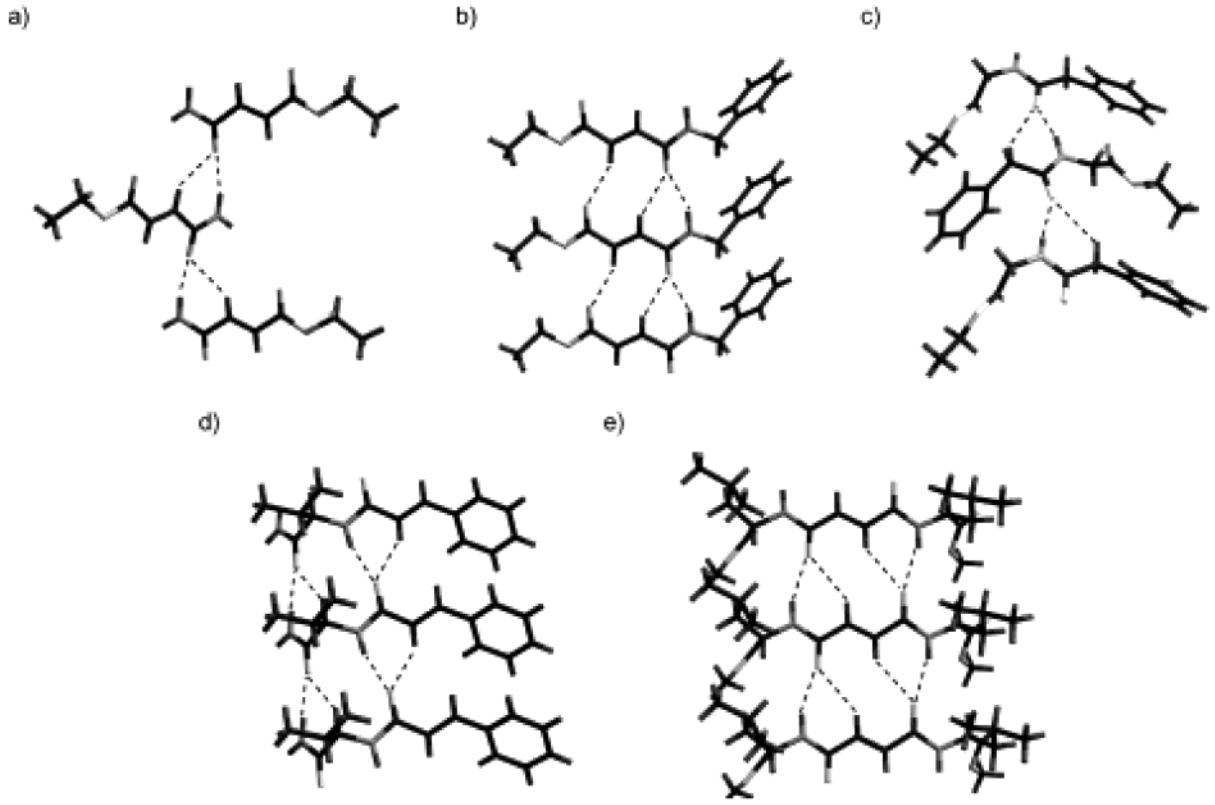

Figure 5. Diagrams illustrating the intermolecular packing interactions involving hydrogen bonding as found in the X-ray crystal structures of (a) **1**, (b) **2**, (c) **3**, (d) **5**, and (e) **6**.

Table 9. Hydrogen-Bonding Distances and Angles in **1**−**3**, **5**, and **6**

X–H	X···O (Å)	H···O (Å)	∠XH···O (deg)
	1, $Et_2OC-CH_b=CH_a-CONH_2$		
N−H_{anti}	2.90(1)	1.95(1)	170(1)
C−H_a	3.34(1)	2.57(1)	139(1)
	2, $Et_2OC-CH_b=CH_a-CONHCH_2Ph$		
N−H	3.07(1)	2.11(1)	159(1)
C−H_a	3.25(1)	2.42(1)	149(1)
	3, $H_3CH_2CO_2CCH_2NHCOCH_2Ph$		
N−H	2.79(1)	1.90(1)	156(1)
C−H_2	3.45(1)	2.73(1)	131(1)
	5, $Ph-CH_b=CH_a-CONH-CH_c[CH(CH_3)_2]-CONH_2$		
N−*H*	2.97(1)	2.02(1)	152(1)
C−H_a	3.20(1)	2.56(1)	135(1)
N−H_{anti}	2.88(1)	1.91(1)	157(1)
C−H_c	3.31(1)	2.41(1)	141(1)
	(**6**) E-Leu-NHCO−$CH_a=CH_{a'}$−CONH-Leu-E		
N−H	2.96(1)	2.04(1)	156(1)
C−H_a	3.35(1)	2.56(1)	142(1)
N−H	2.95(1)	2.04(1)	162(1)
C−$H_{a'}$	3.32(1)	2.54(1)	138(1)

(secondary) involvement in the intermolecular recognition leading to crystallization.

The NMR study of **3** did not provide evidence of CH···O hydrogen bonding in solution. In the crystal structure of **3**, a short NH···O hydrogen bond [2.79(1) Å] is observed along with a concurrent CH···O hydrogen bond [3.45(1) Å] to one of the two benzylic CHs having a C···O separation near the maximum distance often accepted for these interactions.[8−11] It may be possible that this distance alone prevents a chemical shift change and thus explains our solution results. The CH···O hydrogen bond in **3** may also have less significance for the molecular recognition events during crystal formation than the analogous interactions in **1** and **2**, or it may be an artifact of stronger forces that take over during crystal packing. The data in this study, though consistent and supportive of a weaker CH···O hydrogen bond in **3**, are not sufficient to differentiate these possibilities.

The crystal structure of **5** provides additional support for the importance of concurrent CH···O hydrogen bonds in peptide and protein structure. Three strong hydrogen-bond donors (NHs) and two hydrogen-bond acceptors (amide oxygens) are present in **5** and, as expected on the basis of hydrogen-bonding rules for small molecules,[71,72] each NH is hydrogen-bonded to an amide carbonyl oxygen. Two of the NH···O hydrogen bonds are between molecules related by translation, where the amide carbonyl oxygens also make concurrent CH···O hydrogen bonds to the alkene CH (H_a) and $C^{\alpha}H$ (H_c). The distances for the NH···O and CH···O hydrogen bonds in **5** are similar to the values observed for **1** and **2**. The NH···O hydrogen bond not shown in Figure 5d occurs between the carboxamide and the secondary amide carbonyl oxygen [$NH_{syn}\cdots O_{2°amide}$, N···O separation = 2.99(1) Å, ∠NH···O = 163(1)°]. The ψ torsion angle within the valinamide [134°] is consistent with the angle expected for antiparallel β-sheet structure [135°].[73]

The symmetric fumaric acid derivative **6** forms concurrent NH···O and CH···O hydrogen bonds in the solid state with distances similar to those observed in **1** and **2**. The melting point

(70) Arnett, E. M.; Mitchell, E. J.; Murty, T. S. S. R. *J. Am. Chem. Soc.* **1974**, *96*, 3875−3891.
(71) Etter, M. C. *J. Phys. Chem.* **1991**, *95*, 4601−4610.
(72) Etter, M. C. *Acc. Chem. Res.* **1990**, *23*, 120−126.
(73) Creighton, T. E. *Proteins, Structure and Molecular Properties*, 2nd ed.; W. H. Freeman: New York, 1984; p 183.

of **6** (202−204 °C) is significantly higher in comparison to **7** (106−108 °C), though it is possible that **7** adopts a folded solid-state conformation, on the basis of the X-ray structures of ring-constrained analogues.[74]

The CH···O hydrogen bonds in these crystal structures can be defined as either attractive and stabilizing, repulsive and stabilizing, or repulsive and destabilizing.[8,75] It is reasonable to expected that the interactions are stabilizing, but it is not possible to know whether they are attractive or repulsive in the solid state. Other intermolecular forces such as NH···O hydrogen bonds or aromatic ring interactions with themselves or other functional groups may influence the CH···O hydrogen bond and manifest these influences on the distances and angles associated with the CH···O contact. Indeed, significant energy is associated with the solid-state packing of aromatic rings[75] and the interaction of aromatic rings with π-CHs has also been shown to influence conformation in small molecules.[76,77] The evidence for participation by the various C−H groups in the DMSO-d_6 titrations is consistent with the observation of similar solid-state CH···O hydrogen bonds, although definitive assignments of alkene chemical shifts in **1** and **2** were not made in these experiments.

Conclusion

The formation of a CH···O hydrogen bond concurrent with NH···O hydrogen bonding is a motif previously reported to occur in the solid-state cocrystal between barbital and acetamide.[78,79] Replacement of a NH···O hydrogen bond with a CH···O hydrogen bond within the context of an intermolecular dimer has reported[80] that could thereby serve as an isofunctional replacement for some NH···O hydrogen bonds. The participation of C−H groups in hydrogen bonding warrants further empirical studies aimed at determining the strength of these interactions, thereby better understanding their contributions to molecular recognition and protein structure. In this way, the fumaramides and related compounds represent models of the *N*-acylpeptide bond that are useful for both solution and solid-state studies of CH···O hydrogen bonds.

Experimental Section

General Methods. All apparatus were oven-dried and cooled in a desiccator. Reagent-grade THF and CH_2Cl_2 were distilled from sodium benzophenone ketyl and CaH_2, respectively, before use. An ammonia in THF solution was prepared by condensing gaseous ammonia to yield an approximate 30% (v/v) solution in THF. Diethyl fumarate and all other reagents were purchased from commercial suppliers and used without purification. Thin-layer chromatography was performed on Analtech 250 μm silica gel HLF Uniplates and were visualized with UV, I_2, and ninhydrin spray for amines. Melting points were obtained on a Fisher-Johns melting point apparatus and are uncorrected. Elemental analyses were performed by Desert Analytics in Phoenix, AZ. ^{1}H and ^{13}C NMR spectra were measured at 400 and 50.3 MHz, respectively, either in $CDCl_3$, with $CHCl_3$ as the internal reference for ^{1}H (δ 7.26) and $CDCl_3$ as the internal reference for ^{13}C (δ 77.06), or in DMSO-d_6, with DMSO as the internal reference for ^{1}H (δ 2.50) and DMSO-d_6 as the internal reference for ^{13}C (δ 39.50). For **5**, a small volume of MeOH-d_4 was added to the $CDCl_3$ in order to aid solubility.

4-Amino-4-oxo-(*E*)-2-butenoic Acid Ethyl Ester (1). Monoethyl fumarate (0.200 g, 1.39 mmol) was added to 10 mL of benzene, thionyl chloride (0.10 mL, 1.37 mmol)) was added dropwise with stirring, and the resulting solution was refluxed for 12 h. The solvents were removed under vacuum, and residual $SOCl_2$ was removed by azeotropic formation with added CH_2Cl_2 (3×) that was removed under vacuum. The resulting oil was dissolved in THF, and 0.40 mL of ammonia in THF (∼30% v/v) was added dropwise at 0 °C. The reaction was stirred for 5 min at room temperature before removal of THF under vacuum. The resulting material was partitioned between EtOAc and a 10% citric acid solution. The organic fraction was washed consecutively with a 1 M $NaHCO_3$ solution, water, and brine. The solution was dried ($MgSO_4$) and filtered, and the solvent was removed under vacuum to give 0.195 g of **1** (98%). An analytical sample was obtained by crystallization from ethyl acetate/hexanes: mp 91−94 °C [lit. mp 94 °C (ref 81), 93−95 °C (ref 82)]; ^{1}H NMR (10 mM in $CDCl_3$) δ 6.96 (d, J = 15.6 Hz, 1 H), 6.83 (d, J = 15.6 Hz, 1 H), 5.66 (br s, 2 H), 4.26 (q, J = 7.2 Hz, 2 H), 1.32 (t, J = 7.2 Hz, 3 H); ^{1}H NMR (10 mM in DMSO-d_6) δ 7.90 (br s, 1 H), 7.51 (br s, 1 H), 6.96 (d, J = 15.6 Hz, 1 H), 6.56 (d, J = 15.6 Hz, 1 H), 4.18 (q, J = 7.2 Hz, 2 H), 1.24 (t, J = 7.2 Hz, 3 H); ^{13}C NMR ($CDCl_3$) δ 166.2, 165.5, 135.7, 131.3, 61.3, 14.0; FAB MS m/z 144 $[M + H]^+$. Anal. Calcd for $C_6H_9NO_3$: C, 50.34; H, 6.34; N, 9.79. Found: C, 50.09; H, 6.32; N, 9.57.

4-Oxo-4-[(phenylmethyl)amino]-(*E*)-2-butenoic Acid Ethyl Ester (2). Monoethyl fumarate (2.000 g, 13.9 mmol) was added to 100 mL of benzene, thionyl chloride (3.00 mL, 41.1 mmol) was added dropwise with stirringand the resulting solution was refluxed for 17 h. The solvents were removed under vacuum, and residual $SOCl_2$ was removed by azeotropic formation with added CH_2Cl_2 (3×) that was removed under vacuum. The resulting oil was dissolved in toluene and cooled to −78 °C under Ar. A solution of benzylamine (3.04 mL, 27.8 mmol) in toluene was added dropwise and the solution was stirred for 2 h at −78 °C. The toluene was removed under vacuum, and the residue was partitioned between EtOAc and a 10% citric acid solution. The organic fraction was washed consecutively with a 1 M $NaHCO_3$ solution, water, and brine. The solution was dried ($MgSO_4$) and filtered, and the solvent was removed under vacuum to give 1.777 g of **2** (55%). An analytical sample was obtained by crystallization from ethyl acetate/hexanes: mp 109−110 °C; ^{1}H NMR (10 mM in $CDCl_3$) δ 7.24−7.37 (m, 5 H), 6.90 (d, J = 15.6 Hz, 1 H), 6.85 (d, J = 15.6 Hz, 1 H), 6.02 (br s, 1 H), 4.55 (d, J = 5.2 Hz), 4.24 (q, J = 7.2 Hz, 2 H), 1.31 (t, J = 7.2 Hz, 3 H); ^{1}H NMR (10 mM in DMSO-d_6) δ 9.02 (s, 1 H), 7.24−7.35 (m, 5 H), 7.06 (d, J = 15.6 Hz, 1 H), 6.62 (d, J = 15.6 Hz, 1 H), 4.39 (d, J = 6.0 Hz), 4.19 (q, J = 7.2 Hz, 2 H), 1.24 (t, J = 7.2 Hz, 3 H); ^{13}C NMR ($CDCl_3$) δ 165.8, 163.6, 137.4, 136.4, 130.3, 128.7, 127.9, 127.6, 61.1, 43.9, 14.0; FAB MS m/z 234 $[M + H]^+$. Anal. Calcd for $C_{13}H_{15}NO_3$: C, 66.93; H, 6.48; N, 6.01. Found: C, 66.73; H, 6.48; N, 6.01.

N-(Phenylacetyl)glycine Ethyl Ester (3). Phenylacetic acid (2.000 g, 14.7 mmol) was added to 100 mL of benzene, thionyl chloride (2.14 mL, 29.4 mmol) was added dropwise with stirring, and the resulting solution was refluxed for 22 h. The solvents were removed under vacuum, and residual $SOCl_2$ was removed by azeotropic formation with added CH_2Cl_2 (3×) that was removed under vacuum. The resulting oil was dissolved in THF and added dropwise to a solution containing glycine ethyl ester hydrochloride (4.10 g, 29.4 mmol) and diisopropylethylamine (5.12 mL, 29.4 mmol) in THF. After 20 min at room temperature, the THF was removed under vacuum and the residue was partitioned between EtOAc and a 10% citric acid solution. The organic fraction was washed consecutively with a 1 M $NaHCO_3$ solution, water,

(74) Ranganathan, D.; Haridas, V.; Kurur, S.; Thomas, A.; Madhusudanan, K. P.; Nagaraj, R.; Kunwar, A. C.; Sarma, A. V. S.; Karle, I. L. *J. Am. Chem. Soc.* **1998**, *120*, 8448−8460.
(75) Dunitz, J. D.; Gavezzotti, A. *Acc. Chem. Res.* **1999**, *32*, 677−684.
(76) Jennings, W. B.; Farrell, B. M.; Malone, J. F. *Acc. Chem. Res.* **2001**, *34*, 885−894.
(77) Tóth, G.; Murphy, R. F.; Lovas, S. *Protein Eng.* **2001**, *14*, 543−547.
(78) Berkovitch-Yellin, Z.; Leiserowitz, L. *J. Am. Chem. Soc.* **1980**, *102*, 7677−7690.
(79) Berkovitch-Yellin, Z.; Leiserowitz, L. *Acta Crystallogr., Sect. B.* **1984**, *40*, 159−165.
(80) Schuck, C.; Lex, J. *Eur. J. Org. Chem.* **2001**, 1519−1523.
(81) Loubinoux, B.; Gérardin, P.; Kunz, W.; Herzog, J. *Pestic. Sci.* **1991**, *33*, 263−269.
(82) Quirós, M.; Astorga, C.; Rebolledo, F.; Gotor, V. *Tetrahedron* **1995**, *51*, 7715−7720.

and brine. The solution was dried ($MgSO_4$) and filtered, and the solvent was removed under vacuum to give 0.342 g of **3** (11%). An analytical sample was obtained by dissolving the product in EtOAc and allowing the solution to diffuse against hexanes: mp 79−82 °C [lit. mp 82 °C (ref 83)]; ^{1}H NMR (10 mM in $CDCl_3$) δ 7.24−7.39 (m, 5 H), 5.89 (br s, 1 H), 4.18 (q, J = 7.2 Hz, 2 H), 4.00 (d, J = 4.8 Hz, 2 H), 3.63 (s, 2 H), 1.26 (t, J = 7.2 Hz, 3 H); ^{1}H NMR (10 mM in DMSO-d_6) δ 8.46 (s, 1 H), 7.21−7.29 (m, 5 H), 4.07 (q, J = 7.2 Hz, 2 H), 3.82 (d, J = 5.6 Hz, 2 H), 3.40−3.51 (m, 2 H), 1.17 (t, J = 7.2 Hz, 3 H); ^{13}C NMR ($CDCl_3$) δ 171.1, 169.7, 134.4, 129.4, 129.0, 127.4, 61.5, 43.4, 41.4, 14.0; FAB MS m/z 222 $[M + H]^+$; Anal. Calcd for $C_{12}H_{15}NO_3$: C, 65.14; H, 6.83; N, 6.33. Found: C, 64.99; H, 6.85; N, 6.21.

***N*-[1-Oxo-3-phenyl-2-(*E*)-propenyl]glycine Ethyl Ester (4).** *trans*-Cinnamic acid (1.06 g, 7.16 mmol) was added to 20 mL of an CH_2Cl_2 and glycine ethyl ester hydrochloride (1.000 g, 7.16 mmol), and then diisopropylethylamine (1.25 mL, 7.16 mmol), and 1-[3-(dimethylamino)propyl]-3-ethylcarbodiimide hydrochloride (1.44 g, 7.52 mmol) were added consecutively. After 24 h, another 20 mL of CH_2Cl_2 was added and the solution was extracted with a 10% citric acid solution. The organic fraction was washed consecutively with a 1 M $NaHCO_3$ solution, water, and brine. The solution was dried ($MgSO_4$) and filtered, and the solvent was removed under vacuum to a pale yellow solid. Crystallization from CH_3OH provided 365 mg of **4** (22%): mp 107−108 °C [lit. mp 106−107 °C (ref 63)]; ^{1}H NMR (10 mM in $CDCl_3$) δ 7.66 (d, J = 15.6 Hz, 1 H), 7.51−7.53 (m, 2 H), 7.37−7.41 (m, 3 H), 6.47 (d, J = 15.6 Hz, 1 H), 6.13 (br s, 1 H), 4.26 (q, J = 7.2 Hz, 2 H), 4.18 (d, J = 5.2 Hz, 2 H), 1.31 (t, J = 7.2 Hz, 3 H); ^{1}H NMR (10 mM in DMSO-d_6) δ 8.53 (t, J = 6.0 Hz, 1 H), 7.58−7.60 (m, 2 H), 7.46 (d, J = 16.0 Hz, 1 H), 7.38−7.43 (m, 3 H), 6.72 (d, J = 16.0 Hz, 1 H), 4.12 (q, J = 7.2 Hz, 2 H), 3.96 (d, J = 6.0 Hz, 2 H), 1.21 (t, J = 7.2 Hz, 3 H); ^{13}C NMR ($CDCl_3$) δ 170.1, 166.1, 141.6, 134.5, 129.7, 128.7, 127.8, 119.8, 61.5, 41.5, 14.0; FAB MS m/z 234 $[M + H]^+$. Anal. Calcd for $C_{13}H_{15}NO_3$: C, 66.93; H, 6.48; N, 6.01. Found: C, 67.03; H, 6.45; N, 5.99.

***N*-[1-Oxo-3-phenyl-2-(*E*)-propenyl)-(*S*)-valinamide (5).** *trans*-Cinnamic acid (0.225 g, 1.52 mmol) was added to 5 mL of an ethanol/water (1:1) mix, and then (*S*)-valinamide hydrobromide (0.300 g, 1.52 mmol), *N*-methylmorpholine (0.167 mL, 1.52 mmol), and 1-[3-(dimethylamino)propyl]-3-ethylcarbodiimide hydrochloride (0.291 g, 1.52 mmol) were added consecutively. After 24 h, CH_2Cl_2 (20 mL) was added and the solution was extracted with a 10% citric acid solution. The organic fraction was washed consecutively with a 1 M $NaHCO_3$ solution, water, and brine. The solution was dried ($MgSO_4$) and filtered, and the solvent was removed under vacuum to yield a solid. Crystallization from CH_3OH provided 141 mg of **5** (38%): mp 246−248 °C; $[\alpha]_D$ +32.9 (*c* 0.70, MeOH); ^{1}H NMR ($CDCl_3$/CD_3OD) δ 7.51 (d, J = 15.6 Hz, 1 H), 7.42−7.45 (m, 2 H), 7.27−7.31 (m, 3 H), 6.49 (d, J = 15.6 Hz, 1 H), 1.96−2.05 (m, 1 H), 0.88−0.92 (m, 6 H); ^{13}C NMR (DMSO-d_6) δ 173.0, 164.9, 138.8, 135.1, 129.4, 129.0, 127.5, 122.4, 57.5, 30.6, 19.4, 18.0; FAB MS m/z 247 $[M + H]^+$. Anal. Calcd for $C_{14}H_{18}N_2O_2$: C, 68.27; H, 7.37; N, 11.38. Found: C, 68.26; H, 7.36; N, 11.20.

1,4-Dioxo-2-(*E*)-butene-1,4-diylbis[*N*-(*S*)-leucine Methyl Ester] (6). Fumaric acid (0.096 g, 0.83 mmol) was added to 5 mL of an ethanol/water (1:1) mix, and (*S*)-leucine methyl ester hydrochloride (0.300 g, 1.65 mmol), *N*-methylmorpholine (0.182 mL, 1.65 mmol), and 1-[3-(dimethylamino)propyl]-3-ethylcarbodiimide hydrochloride (0.317 g, 1.65 mmol) were added consecutively. Workup was done as described for **5**. Crystallization from CH_3OH provided 150 mg of **6** (49%): mp 202−204 °C; $[\alpha]_D$ −79.6 (*c* 0.65, MeOH); ^{1}H NMR (10 mM in $CDCl_3$) δ 6.90 (s, 2 H), 6.67 (d, J = 8.0 Hz, 2 H), 4.71−4.76 (m, 2 H), 3.76 (s, 6 H), 1.56−1.72 (m, 6 H), 0.93−0.95 (m, 12 H); ^{1}H NMR (10 mM in DMSO-d_6) δ 8.81 (d, J = 7.2 Hz, 2 H), 6.90 (s, 2 H), 4.34−4.40 (m, 2 H), 3.64 (s, 6 H), 1.50−1.65 (m, 6 H), 0.86−0.92 (m, 12 H); ^{13}C NMR ($CDCl_3$) δ 173.7, 164.3, 133.1, 52.3, 50.9, 40.9, 24.8, 22.8, 21.6; FAB MS m/z 371 $[M + H]^+$. Anal. Calcd for $C_{18}H_{30}N_2O_6$: C, 58.36; H, 8.16; N, 7.56. Found: C, 58.63; H, 7.99; N, 7.47.

1,4-Dioxobutane-1,4-diylbis[*N*-(*S*)-leucine Methyl Ester] (7). The reaction was set up and worked up as described for **6**, starting with 0.096 g (0.83 mmol) of succinic acid. Crystallization from CH_3OH provided 157 mg of **7** (51%): mp 106−108 °C; $[\alpha]_D$ −49.3 (*c* 0.75, MeOH); ^{1}H NMR (10 mM in $CDCl_3$) δ 6.53 (d, J = 7.6 Hz, 2 H), 4.55−4.61 (m, 2 H), 3.73 (s, 6 H), 2.49−2.62 (m, 4 H), 1.50−1.72 (m, 6 H), 0.92−0.94 (m, 12 H); ^{1}H NMR (10 mM in DMSO-d_6) δ 7.21 (d, J = 8.0 Hz, 2 H), 4.51−4.57 (m, 2 H), 3.71 (s, 6 H), 2.52−2.60 (m, 4 H), 1.55−1.69 (m, 6 H), 0.91−0.94 (m, 12 H); ^{13}C NMR ($CDCl_3$) δ 173.8, 172.2, 52.2, 50.9, 40.9, 31.7, 24.7, 22.8, 21.6; FAB MS m/z 373 $[M + H]^+$; Anal. Calcd for $C_{18}H_{32}N_2O_6$: C, 58.04; H, 8.66; N, 7.52. Found: C, 58.28; H, 8.60; N, 7.31.

Screening by Parallel Synthesis. Stock solutions were prepared in EtOH. The monocarboxylic acid and amino acid salts were prepared at 0.250 M, whereas *N*-methylmorpholine in EtOH was prepared at 0.500 M and the dicarboxylic acids were prepared at 0.125 M. Some samples required heating to fully dissolve. A 0.250 M solution of 1-[3-(dimethylamino)propyl]-3-ethylcarbodiimide hydrochloride was freshly prepared in water. The different combinations were prepared by combining 100 μL each of the amino acid salt solution and acid solutions, along with 200 μL of the carbodiimide solution and 75 μL of the *N*-methylmorpholine solution (except for histidine where 150 μL of base was used). The solutions were allowed to react and slowly evaporate at room temperature; they were observed periodically for the formation of crystalline solids. From these experiments, **4**−**7** were identified as crystalline and worth further analysis.

Solution NMR Analysis. Stock solutions at 100 mM were prepared of the compound under analysis in $CDCl_3$ and DMSO-d_6. In addition, a diluted stock (10 mM) in DMSO-d_6 was also prepared. Both NMR solvents contained 0.3% TMS (v/v) as a standard. The stock solutions were used to create the NMR samples for analysis, containing 5, 10, 20, 50, 100, 200, and 500 mM and 1.0 and 10.0 M DMSO-d_6 in $CDCl_3$. Solutions at 10 mM in $CHCl_3$ as well as DMSO-d_6 at 14.1 M that contained trace $CHCl_3$were also prepared. The $CDCl_3$/DMSO-d_6 solutions are uncorrected for any volume differences due to mixing.

X-ray Single-Crystal Diffraction. The crystal data for **1**−**3**, **5**, and **6** were collected on a Siemens P4 four-circle diffractometer equipped with a Bruker SMART 1000 CCD and graphite-monochromated Mo−Kα (λ = 0.710 73 Å) radiation at either 203 or 293 K. The data were integrated with SAINT. Crystal stabilities were monitored by measuring 3 standard reflections after every 97 reflections with no significant decay in observed intensities. A $\theta - 2\theta$ scanning technique was used for peak collection with Lorenz and polarization corrections applied. Hydrogen atom positions were located from difference Fourier maps, and a riding model with fixed thermal parameters [$u_{ij} = 1.2U_{ij}$(eq) for the atom to which they are bonded] was used for subsequent refinements. The weighting function applied was $w^{-1} = [\sigma^2(F_o^2) + (g_1P)^2 + (g_2P)]$, where $P = [F_o^2 + 2F_c^2]/3$. In all structures the SHELXTL PC and SHELXL-93 packages[84] were used for data reduction, structure solution, and refinement.

Acknowledgment. This work was supported in part by NIH−COBRE Award 1-P20-RR15563 with matching support from the state of Kansas and NSF−REU support (0097411) for W.P.-S.

Supporting Information Available: Figures representing the solid-state structures of **1**, **2**, **3**, **5**, and **6** showing the thermal ellipsoids and atom labeling (PDF) and X-ray crystallographic files for **1**, **2**, **3**, **5**, and **6** (CIF). This material is available free of charge via the Internet at http://pubs.acs.org.

JA0257366

(83) Saito, T.; Nishihata, K.; Fukatsu, S. *J. Chem. Soc., Perkin Trans. 1* **1981**, *4*, 1058−1063.
(84) Sheldrick, G. M. SHELXL-93, University of Göttingen, Germany.